EDGEWOOD
RESEARCH, DEVELOPMENT & ENGINEERING CENTER
U.S. ARMY CHEMICAL AND BIOLOGICAL DEFENSE COMMAND

ERDEC-TR-395

BACKSCATTER AND TRANSMISSION OF AEROSOL AT UV THROUGH MIDDLE IR WAVELENGTHS

Hugh R. Carlon, U.S. Army Fellow
Charles H. Wick
RESEARCH AND TECHNOLOGY DIRECTORATE

February 1997

Aberdeen Proving Ground, MD 21010-5423

Disclaimer

The findings in this report are not to be construed as an official Department of the Army position unless so designated by other authorizing documents.

DEPARTMENT OF THE ARMY
U.S. Army Edgewood Research, Development and Engineering Center
Aberdeen Proving Ground, Maryland 21010-5423

ERRATUM SHEET

30 October 1997

REPORT NO.	ERDEC-TR-395
TITLE	BACKSCATTER AND TRANSMISSION OF AEROSOL AT UV THROUGH MIDDLE IR WAVELENGTHS
AUTHORS	Hugh R. Carlon, U.S. Army Fellow, and Charles H. Wick
DATE	February 1997
CLASSIFICATION	UNCLASSIFIED

Please remove the front cover from copies of ERDEC-TR-395 sent to you earlier in 1997 and attach the enclosed replacement cover. Previously printed covers were inadvertently printed with the incorrect activity name and logo.

Sandra J. Johnson
SANDRA J. JOHNSON
Chief, Technical Releases Office

REPORT DOCUMENTATION PAGE

Form Approved
OMB No. 0704-0188

1. AGENCY USE ONLY *(Leave Blank)*	2. REPORT DATE	3. REPORT TYPE AND DATES COVERED
	1997 February	Final; 92 Sep - 94 Jun

4. TITLE AND SUBTITLE
Backscatter and Transmission of Aerosol at UV Through Middle IR Wavelengths

5. FUNDING NUMBERS
C-DAJA45-92-C-0024

6. AUTHOR(S)
Carlon, Hugh R., U.S. Army Fellow, and Wick, Charles, H.

7. PERFORMING ORGANIZATION NAME(S) AND ADDRESS(ES)
DIR, ERDEC, ATTN: SCBRD-RTE, APG, MD 21010-5423

8. PERFORMING ORGANIZATION REPORT NUMBER
ERDEC-TR-395

9. SPONSORING/MONITORING AGENCY NAME(S) AND ADDRESS(ES)

10. SPONSORING/MONITORING AGENCY REPORT NUMBER

11. SUPPLEMENTARY NOTES

12a. DISTRIBUTION/AVAILABILITY STATEMENT
Approved for public release; distribution is unlimited.

12b. DISTRIBUTION CODE

13. ABSTRACT *(Maximum 200 words)*
A Continuum Surelite 10 Hz Nd:Yag laser system was purchased for these measurements. It included second, third, and fourth harmonic generators. After setup, beam profiles were made, and the apparatus was configured to measure backscatter and extinction of laser radiation due to aerosol and cloud polydispersions. Simultaneous measurements of backscatter and transmission coefficients for obscuring carbon and biological aerosols were investigated in the laboratory at wavelengths of 1064, 532, 355, and 266 nm. Water clouds also were well-characterized.

14. SUBJECT TERMS
Backscatter
Transmission
ND:Yag laser
Obscuring aerosols
Biological aerosol
Spores
Pollen

15. NUMBER OF PAGES
25

16. PRICE CODE

17. SECURITY CLASSIFICATION OF REPORT	18. SECURITY CLASSIFICATION OF THIS PAGE	19. SECURITY CLASSIFICATION OF ABSTRACT	20. LIMITATION OF ABSTRACT
UNCLASSIFIED	UNCLASSIFIED	UNCLASSIFIED	UL

Blank

PREFACE

The work described in this report was performed as part of Contract No. DAJA45-92-C-0024. This work was started in September 1992 and completed in June 1994.

The use of trade or manufacturers' names in this report does not constitute an official endorsement of any commercial products. This report may not be cited for purposes of advertisement.

This report has been approved for public release. Registered users should request additional copies for the Defense Technical Information Center; unregistered users should direct such requests to the National Technical Information Service.

Acknowledgments

The work reported here was funded by Steven Gotoff, U.S. Army Edgewood Research, Development and Engineering Center (ERDEC), through the U.S. Army European Research Office, under the astute guidance of Jerry Comati, Chief, Environmental Sciences Branch. Dr. Gerard Jennings, University College, Galway, Ireland, was the principal investigator. Although only informal reports documenting his research were required, he gave specific written permission to the authors to interpret and preserve his important work in a formal ERDEC technical report. He also asked that authorship of the report be vested in ERDEC in recognition of the effort required and the long collaborative history involving ERDEC scientists and the Galway staff. The outstanding research of Dr. R.E.C. Jennings in the transmission and backscatter measurements at Galway deserves special recognition.

Blank

CONTENTS

FIGURES

TABLES

BACKSCATTER AND TRANSMISSION OF AEROSOL

AT UV THROUGH MIDDLE IR WAVELENGTHS

1. INTRODUCTION

This report describes backscatter and transmission measurements using a Nd:Yag pulsed laser system operating at its fundamental wavelength and its harmonics.

The experiments have been designed to measure both backscatter and transmission for obscuring aerosols and biological aerosols in the laboratory. The experimental equipment was first tested for absorbing aerosol clouds (Asbury M260 Graphite Powder). Later this same set up was extended to characterize biological aerosols such as pollens.

2. EXPERIMENTAL PROCEDURE

Photoelectric probes from Molectron were used to detect the transmitted and backscattered energies from a Continuum Surelite Nd:Yag pulsed laser system. The nominal maximum energies of the Continuum Surelite laser are 365 nJ at the fundamental wavelength of 1064 nm, 165 mJ at the second harmonic wavelength of 532 nm, 55 mJ at the third and fourth harmonic wavelengths of 355 and 266 nm. The pyroelectric probes were capable of withstanding the energy densities and have fast response times (up to 50 pulses per second) enabling single or multiple laser shots at 10 or 20 Hz to be used. This is a considerable advantage over the slow response volumetric detection probes which only allow single shots to be measured.

The J50 probe with beam expander (JBX) enabled the higher transmitted energies to be detected in the range uJ to J. The J4 - 09 probe enabled the lower backscattered energies to be measured in the range 50 nJ to 5 mJ.

A dual channel power/energy meter (JD 2000 from Molectron) has been calibrated for the two probes to measure the energy (or power) directly (A and B) and also gives direct readings A/B, B/A and the average over 1 to 100 slots (with standard deviation). The ability to use both probes simultaneously (at 10 Hz in present measurements) means that any fluctuations in the aerosol cloud and resulting signals are less significant. The meter is triggered directly from the laser power supply.

A 50 mm diameter circular plano-plano optic (10 mm thickness) made from fused silica with an 8 mm diameter hole bored through it at an angle of 45 degrees centred onto a highly reflecting face is used. Ultra high energy coatings on both surfaces have damage thresholds of 2J in 1 ns at 1064 and 532 nm. The reflecting face has greater than 99.5% reflectance. Hence this mirror is suitable for use with the Continuum Surelite Nd:Yag laser at 1064 and 532 nm.

A schematic diagram of the experimental arrangement is shown in Figure 1. The laser beam was set up to pass through the mirror hole into the aerosol chamber. The transmitted beam was measured directly by the pyroelectric probe. The backscattered signal was reflected immediately below the mirror hole onto the pyroelectric probe. This setup has the advantage that this probe is not damaged by the laser main beam (as it is well away from it) yet can measure backscatter signals at an angle of 0.3° from the far end of the aerosol chamber to 2° from the near end of the aerosol chamber under the existing experimental arrangement.

Two black boxes were designed to give multiple (>20) internal reflections from black mat surfaces to reduce any stray signals from them. One was positioned behind the mirror (opposite side to the probe) and was particularly useful when setting up to absorb any clipped signal. The other movable black box at the far end beyond the cloud chamber was

The system was first tested using well characterised water cloud. The chamber consisted of a box 1.5 m in length lined with black matte felt which was saturated with water during experiments to keep the cloud stable. Shutters at each end of the box were opened when measurements were made. An air jet was directed across the chamber opening to prevent any cloud escaping back onto the optics.

The cloud was generated either by a DeVilbiss Nebuliser situated immediately above the cloud chamber or by up to three humidifiers situated immediately below the cloud chamber, or a combination of these.

The number and size of water droplets was measured using a Particle Measuring System (PMS) classical scattering aerosol spectrometer probe (XCSASP) which can sense water droplets with radii from 0.23 to 14 um. The cloud was checked for stability, repeatability and homogeneity by taking measurements in different places within the cloud at different times using the same cloud generating methods. The histograms for number and size of water droplets were within 14% for similar cloud generating systems. The majority of water droplets using the Nebuliser had radii between 1 and 3.6um (peaking between 1.5 and 2.4 um). The majority of water droplets using the humidifiers, had radii between 0.4 and 2.5 um (peaking between 0.4 and 0.48 um and with a large peak between 1 and 2 um).

3. EXTINCTION AND BACKSCATTER MEASUREMENTS

Extinction measurements have been made at all four wavelengths (1064, 532, 355 and 266 nm). Simultaneous extinction and backscatter measurements have been made at 1064 and 532 nm.

The volume extinction coefficient σ_e is derived from the Lambert-Bouguer expression:

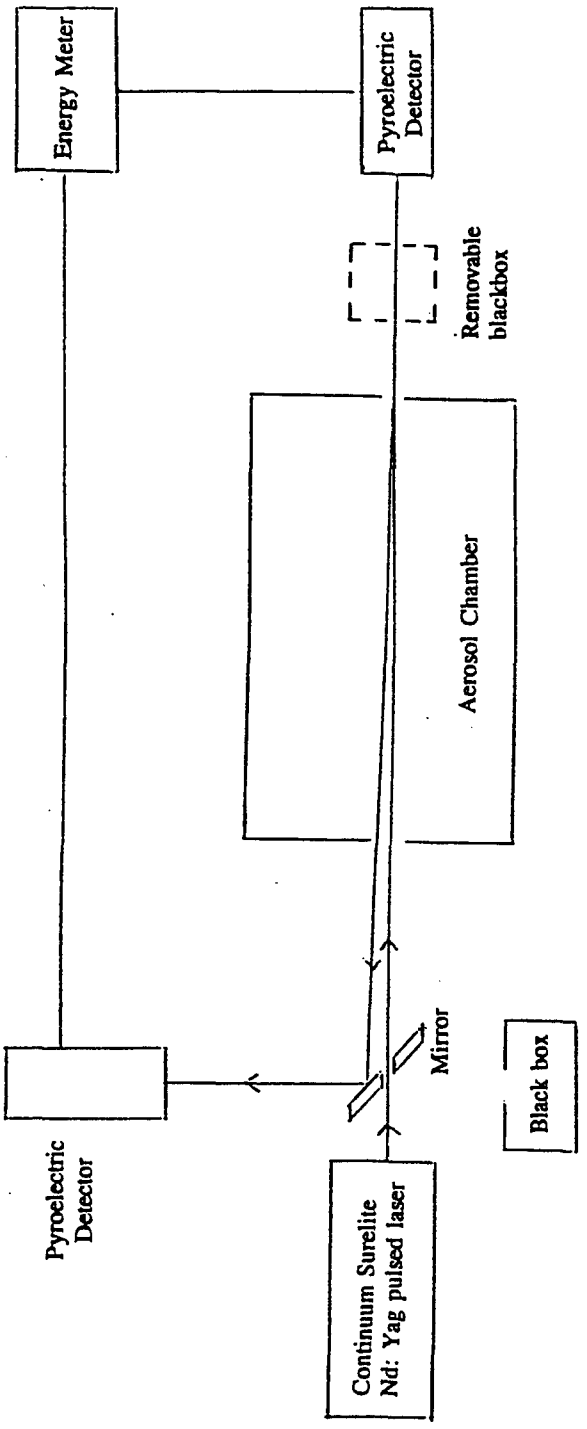

Figure 1. Schematic Diagram of the Experimental Arrangement for Simultaneous Measurements of Transmission and Backscatter.

$$I = I_o \exp(-\sigma_e L) \tag{1}$$

where I is the transmitted signal after traversal through cloud of path length L and I_o is the initial intensity of the laser radiation in the absence of a cloud.

The volume backscatter coefficient, σ_b, is obtained from the expression

$$I_b = I_o \sigma_b A \int_b^{b+L} \frac{\exp(-2\sigma_e l)}{l^2}\, dl \tag{2}$$

where I_b is the measured backscatter signal
A is the detector area
b is the path length between the detector and chamber entrance.

For a particular value of σ_e

$$K = \int_b^{b+L} \frac{\exp(-2\sigma_e l)}{l^2} dl$$

$$K = \frac{\exp(-2\sigma_e b)}{b} - \frac{\exp[-2\sigma_e (b+L)]}{b+L}$$

$$- 2\sigma_e \left\{ \log_e \left(\frac{b+L}{b} \right) - \sum_{n=1}^{\infty} (-1)^{n+1} \frac{2^n \sigma_e^n}{n.n!} [(b+L)^n - b^n] \right\}$$

Considering series $\sum (-1)^{n+1} \frac{2^n \sigma_e^n}{n.n!} [(b+L)^n - b^n]$

$$\frac{(n+1)^{th}\ term}{n^{th}\ term} = -\frac{2\sigma_e n}{(n+1)^2} (b+L) \frac{\left\{ 1 - \left(\frac{b}{L+b} \right)^{n+1} \right\}}{\left\{ 1 - \left(\frac{b}{L+b} \right)^{n} \right\}}$$

$$\rightarrow \frac{2\sigma_e (b+L)}{n} \quad \text{for large } n \rightarrow 0$$

Therefore the sum is convergent, so K can be computed and σ_b obtained.

The results for the volume extinction coefficient, σ_e, and the volume backscatter coefficient, σ_b, together with the ratio σ_e/σ_b are given in Table 1 for water droplets at 1064 nm. Fairly good agreement with the theoretical value of $\sigma_e = 18.2\ \sigma_b$ is obtained.

At 1064 nm $\sigma_e = (14.4 \pm 0.4)\ \sigma_b$

At 532 nm $\sigma_b = (53.1 \pm 3.2)\sigma_b$

Hence the measurements have shown that the experimental set up gives good agreement with theory at 1064 nm. Measurements will be made at the other wavelengths and then measurements on Astbury M260 obscuring graphite powder and biological aerosols will be made.

4. FORWARD SCATTERING MEASUREMENTS

The laboratory measurements continued at this point with forward scattering investigations using the Nd:Yag pulsed laser system at its fundamental and 2nd harmonic wavelengths, and with preparation of the experimental arrangements for the generation of obscuring aerosol (Asbury M260 graphite powder).

When a beam of light is passed through an aerosol, light is scattered in all directions by the aerosol. Some light is scattered in the forward direction and enters the aperture of the detector together with the main beam. Hence, a correction to the extinction measurements is required. Similarly since the volumetric backscatter coefficient is a function of the volumetric extinction coefficient any correction in the extinction coefficient will affect backscatter coefficient.

Whilst theoretical predictions of the correction due to forward scattering have been made for both monodisperse and polydisperse aerosols (Deepak and Box, 1978), no published experimental measurements have come to our attention.

The theoretical correction due to forward scattering is a function of wavelength, particle size distribution, real and imaginary components of the complex refractive index and experimental geometry (length of aerosol cloud chamber and distance from aerosol cloud to detector). Firstly, the forward scattering measurements were carried out for a well characterised water cloud (generated by a DeVilbiss Nebuliser or up to three humidifiers or a combination of these).

The experimental arrangement for measuring forward scattering in the laboratory is essentially the same as that for measuring backscattering. However in this case the mirror (with hole in it) is on the far side of the aerosol chamber (instead of near side) as shown in Figure 2. The forward scattered light is reflected from the surface of the mirror immediately adjacent to the hole. In the experimental arrangement the half angle subtended by the detector was < 1° (0.96° from the near end of the aerosol chamber and 0.123° from the far end of the aerosol chamber).

Table 1

Volumetric extinction coefficient, σe, and volumetric backscatter coefficient, σb ,and their ratio $\sigma e/\sigma b$ for cloud water droplets at wavelength 1064 nm.

Cloud Generator	σe(m^-1)	σb(m^-1sr^-1)	$\sigma e/\sigma b$ (sr)
Humidifiers	0.944	8.55 x 10-2	11.0
	0.956	9.18 x 10-2	10.4
	0.982	9.35 x 10-2	10.5
	0.865	6.65 x 10-2	13.0
	0.819	6.13 x 10-2	13.4
	0.819	6.02 x 10-2	13.6
	0.536	2.94 x 10-2	18.2
	0.547	3.20 x 10-2	17.1
	0.494	2.84 x 10-2	17.4
	0.539	3.16 x 10-2	17.1
	0.939	7.77 x 10-2	12.1
	0.766	6.88 x 10-2	11.1
	0.653	3.98 x 10-2	16.4
	0.447	2.53 x 10-2	17.7
	0.345	1.98 x 10-2	17.4
	0.756	5.45 x 10-2	13.9
	0.493	3.16 x 10-2	15.5
	0.567	3.54 x 10-2	16.0
	0.811	6.34 x 10-2	12.8
	0.538	3.41 x 10-2	X5.7
	0.558	3.64 x 10-2	15.2
	0.438	2.91 x 10-2	15.0
	0.421	2.70 x 10-2	15.6
	0.259	2.16 x 10-2	12.0
Humidifiers and Nebulizer	0.665	4.52 x 10-2	14.7
	0.565	4.18 x 10-2	13.5
	0.533	3.84 x 10-2	13.9
	0.534	3.61 x 10-2	14.8
Nebulizer	0.970	7.44 x 10-2	13.0
	0.718	5.38 x 10-2	13.4
	0.527	3 40 x 10-2	15.5
	0.414	2.80 x 10-2	14.8
	0.330	2.33 x 10-2	14.2

The results are shown in Table 2, which gives the ratio, F, of the forward scattered signal to the extinction signal for different clouds of water droplets together with extinction coefficients at 532 and 1064 nm.

Theoretical predictions for F, (the ratio of forward scattered signal to the actual extinction signal unaffected by forward scattered radiation) by a cloud of water droplets of radius are given in Table 3. Three theoretical cases are considered, namely, a monodisperse cloud and two Deirmendjian models for polydisperse aerosol size distributions. These are given by n(r) = r^8 exp (-(br)^3), where the mode radius rm = (8/3)^1/3 b^-1, which represents a relatively narrow distribution and n(r) = r^2 exp (-2r/rm), which represents a broader type distribution.

Table 2 Ratio of forward scattered signal to the true extinction signal (measured extinction signal less the forward scattered signal), F, for different clouds of water droplets for a range of true extinction coefficients.

		Range of σ (m^{-1})	F(%)
(a)	at 1064nm	0.5 → 1.0	3.59 ± 0.17
		1.0 → 3.25	2.41 ± 0.71
(b)	at 532nm	0 → 0.5	0.50 ± 0.07
		0.5 → 1.0	1.00 ± 0.21
		1.0 → 1.75	0.74 ± 0.07

Table 3 Theoretical predictions for F, due to forward scattering by cloud of water droplets of radius assuming (a) monodisperse cloud, (b) polydisperse cloud with size distribution, $n(r) = r^8 \exp(-(br)^3)$ where the mode radius $r_m = (8/3)^{1/3} b^{-1}$ and (c) polydisperse cloud with $n(r) = r^2 \exp(-2r/r_m)$.

Wavelength	Mode radius	F(%)		
(nm)	(μm)	(a)	(b)	(c)
1064	2	1	9	23
	1.5	0.5	6	18
	1	0.3	3	11
532	2	3	3	11
	1.5	1.5	2	8
	1	1	0.5	4

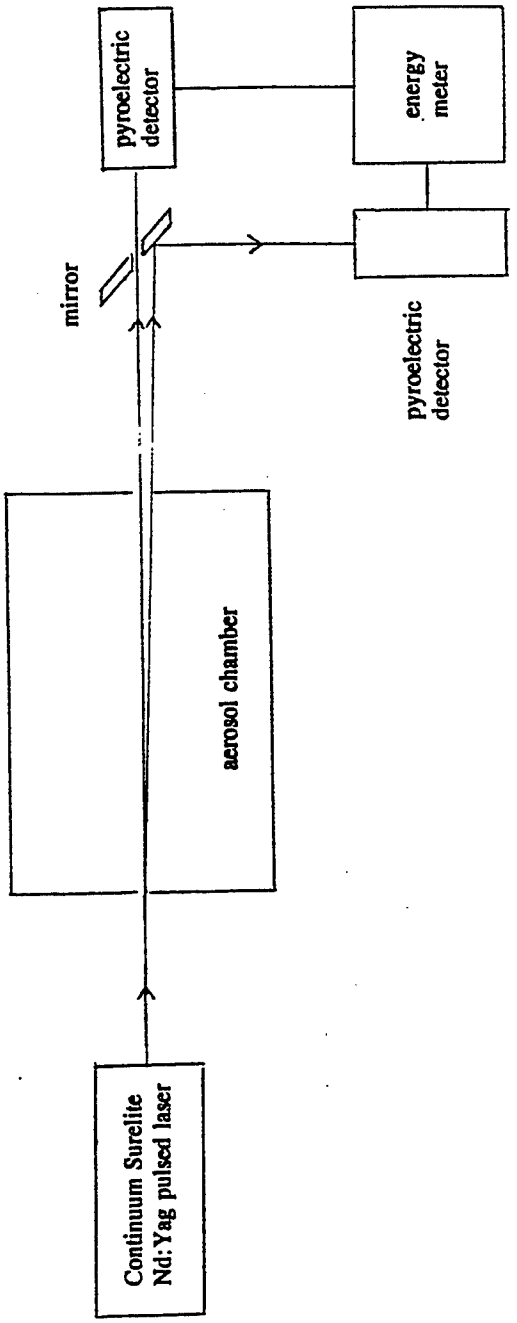

Figure 2. Schematic Diagram of the Experimental Arrangement for Measuring Forward Scattering.

Good agreement is found between the theoretical values obtained for the aerosol size distribution n(r) = r8 exp(-(br3) and those obtained experimentally, on comparing Tables 2 and 3. The theoretical predictions for a monodispersion and the broader dispersion (n(r) = r2 exp (-2r/rm)) are included to demonstrate that forward scattering by aerosols may be significant and should be considered in all exctinction and backscatter measurements.

Forward scattering measurements together with extinction and backscatter measurements were also carried out at 355 and 266 nm and at all four wavelengths (1064, 532, 355 and 266 nm) for obscuring aerosol (Asbury M260 graphite powder).

The aerosol chamber for measuring transmission and backscatter of obscuring aerosol (Asbury M260 graphite powder) is shown in cross-section in Figure 3. A raised floor in the chamber had a systematic array of small air orifices. The four edges of the raised floor were angles up to 45 degrees (with air orifices in them) in order to help contain the aerosol within the chamber. The aerosol was injected near the top of the chamber. A filtered air supply blew air in under the raised floor through the holes and was adjusted to keep the aerosol in suspension in the upward air flow. In this way a stable cloud of aerosol was obtained.

In addition, two separate jets of filtered air were directed at an angle of 45° upward across the laser beam entrance and exit holes to prevent the aerosol escaping from the chamber (Figure 3). The air from the chamber was collected in a large velostat bag. The Continuum Surelite Nd:Yag pulsed laser was used at its fundamental (1065 nm) and harmonic (532, 355 and 266 nm) wavelengths. Simultaneous measurements of transmission and backscatter were made using the same experimental arrangement as described earlier in the present report.

Preliminary experiments were carried out to investigate the aerosol of carbon graphite flakes (Asbury M260 # 4676) generated in the aerosol chamber. A continuous power He-Ne laser (632.8 nm wavelength) was directed through the 1 m long aerosol chamber shown in Figure 4. Filtered air jets were blown at an angle of 45° across the 3/8" diameter entrance and exit holes for the laser in order to contain the aerosol within the chamber. Another filtered air jet blew in the carbon graphite aerosol horizontally a distance 3 cm below the top of the chamber which then was allowed to fall 21 cm under gravity to the laser beam path.

The aerosol was collected in a 1.3 cu m air-tight Velostat conducting bag. The carbon graphite aesosol was investigated for different aerosol clouds by measuring the extinction of the He-Ne laser as a function of time using a photodiode detector and readout meter. The decay in extinction coefficient , σe, with time for carbon graphite aerosol clouds is shown in Figure 5. The initial decay time constant was between 2.7 and 4.7 minutes followed by a slower decay. This is consistent with the given deposition velocities of 0.120 cm/sec and 0.069 cm/sec which yield deposition times of 2.9 and 5.1 respectively in the present setup.

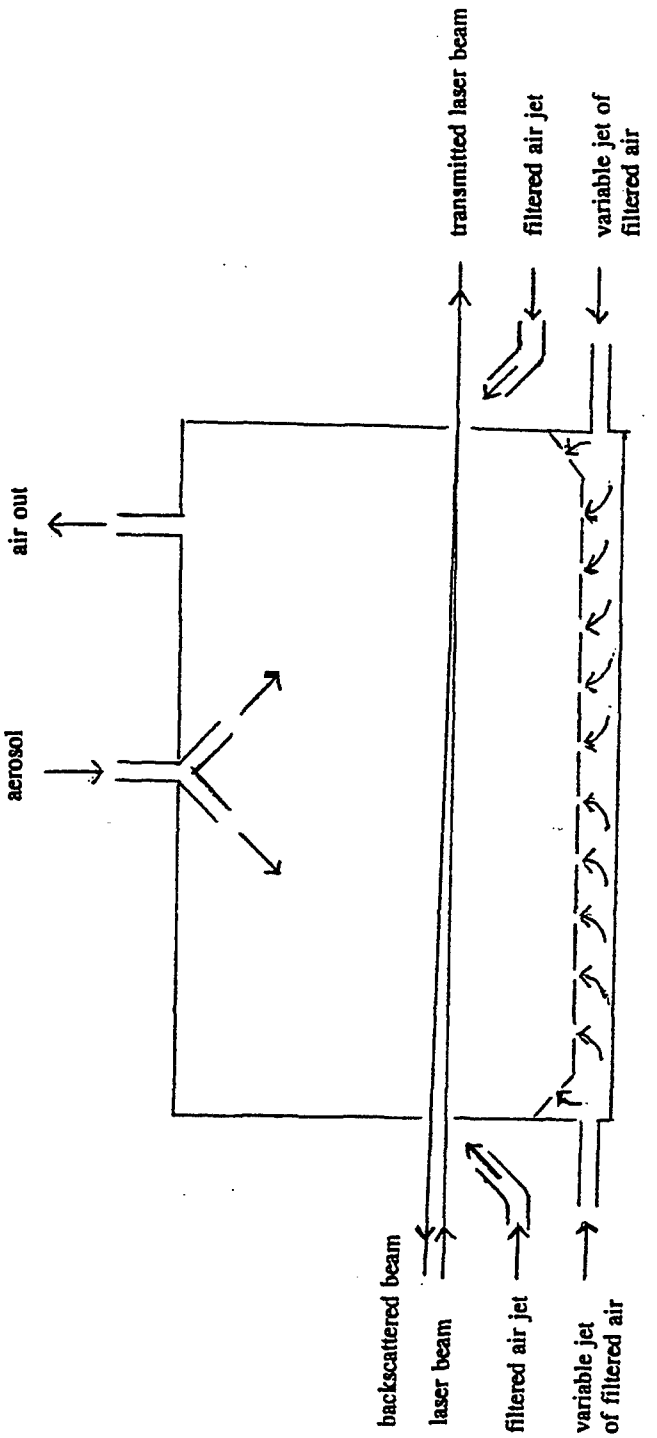

Figure 3. Chamber for Measuring Transmission and Backscatter of Graphite Powder Aerosol.

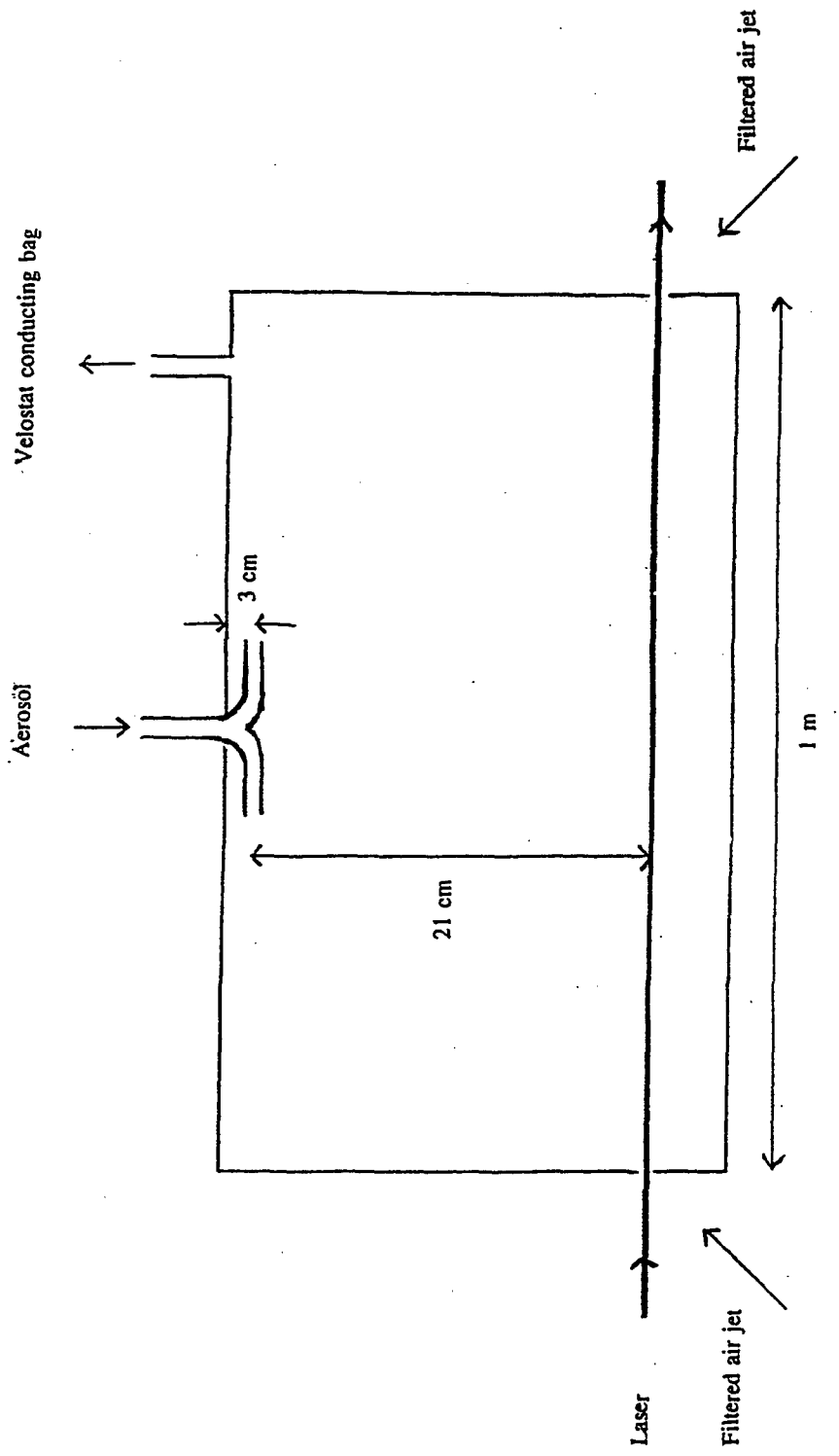

Figure 4. Schematic Diagram of Aerosol Chamber for Carbon Graphite Flakes (Asbury M260, #4676).

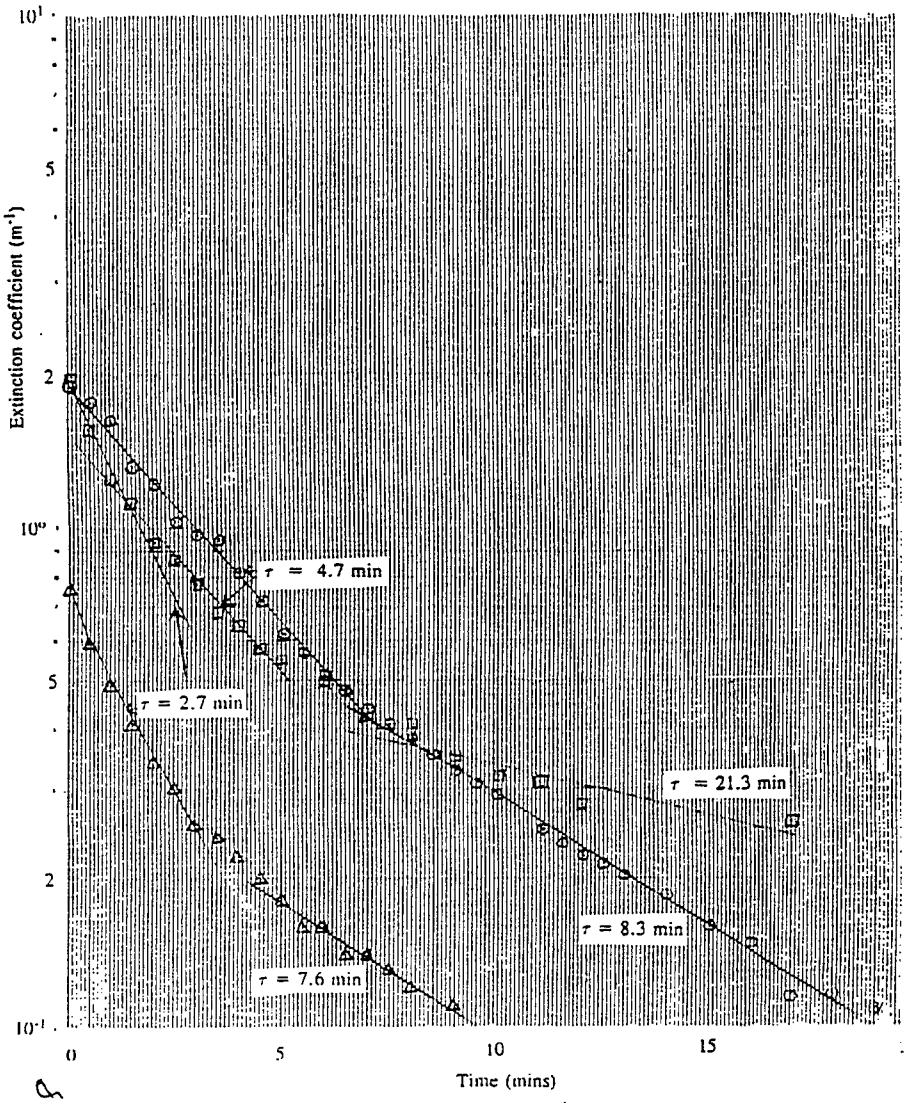

Figure 5. Experimental Decay in Extinction Coefficient with Time for Aerosols of Carbon Graphite Flakes (Asbury M260, #4676).

Laboratory measurements of simultaneous backscatter and transmission for obscuring aerosols of carbon graphite flakes (Asbury M260 #4676) were made using the experimental arrangement shown in Figure 6. A Continuum Surelite Nd:YAG pulsed laser was used at its fundamental 1064 nm wavelength and at its harmonic wavelengths of 532, 355 and 266 nm. The same 1 m aerosol chamber was used as in the preliminary experiment apart from the requirement of larger entrance and exit holes (3.2 and 2.5 cm diameter respectively) for the laser, the holes being plugged when not in use. The larger holes were required: (1) because of the larger diameter of the Nd:YAG laser beam (6 mm diameter); (2) in order to eliminate edge effects from the 8 mm diameter hole in the mirror; (3) in order to obtain all the backscattered signal from the aerosol over the solid angle reflected by the mirror onto the detector (see Figure 6).

The laser beam passed through a hole at 45° through an appropriate wavelength matched high reflectance mirror (> 99.5% reflectance). The backscattered signal was reflected onto the detector from immediately below the hole in the mirror so that the backscattered signal was as close to 180° as possible with the main beam, in this case between 0.3 and 2° from 180°. The extinction and backscattered signals were measured simultaneously by Molectron pyroelectric detectors J50 + JBX and J4-09 respectively. All measurements averaged 10 pulses and were made during cloud decay conditions. The cloud dissipated in 3 or 4 minutes as before, but the longer aerosol decay times were not observed due to the aerosol being blown away by incoming air jets. The values for volume extinction coefficient, σe, and volume backscatter coefficient, σb, were derived from the extinction and backscattered signals.

Great care was taken to reduce the background signal as much as possible because of the low values of backscattered signal. When the J409 detector was displaced, the background noise was not measurable (< 5 x 10-9J). When the J4-09 detector was aligned to measure the backscattered signal a significant signal (about 1 x 10-7J depending on wavelength) was observed due to reflection from the far end of the chamber and the detector. This background signal, Ib, was assumed to be attenuated by the aerosol by an amount given by:

(3) $$Ib = Ibo \exp(-2\sigma eL)$$

where Ibo is the background signal with no aerosol present, and L is the chamber length.

In all measurements Ib was subtracted from the measured backscattered signal to give the true signal due to the aerosol.

The size distribution of the carbon graphite flakes (Asbury M260 # 4676) was analysed using the given data for mass distribution as a function of diameter. The number distribution n(r) was obtained assuming the particles were spherical. Plots of dn(r)/dlog10r against radius, r, and of mass distribution dm(r)/dlog10r against r, showed a

lognormal distribution with a geometric mean radius, rg, of 1.25 um and geometric volume radius, rv, of 2.62 um. On log probability paper, radius vs. cumulative mass was linear up to 90% mass, and at 50% cumulative mass reading the value of rv was 2.65 um.

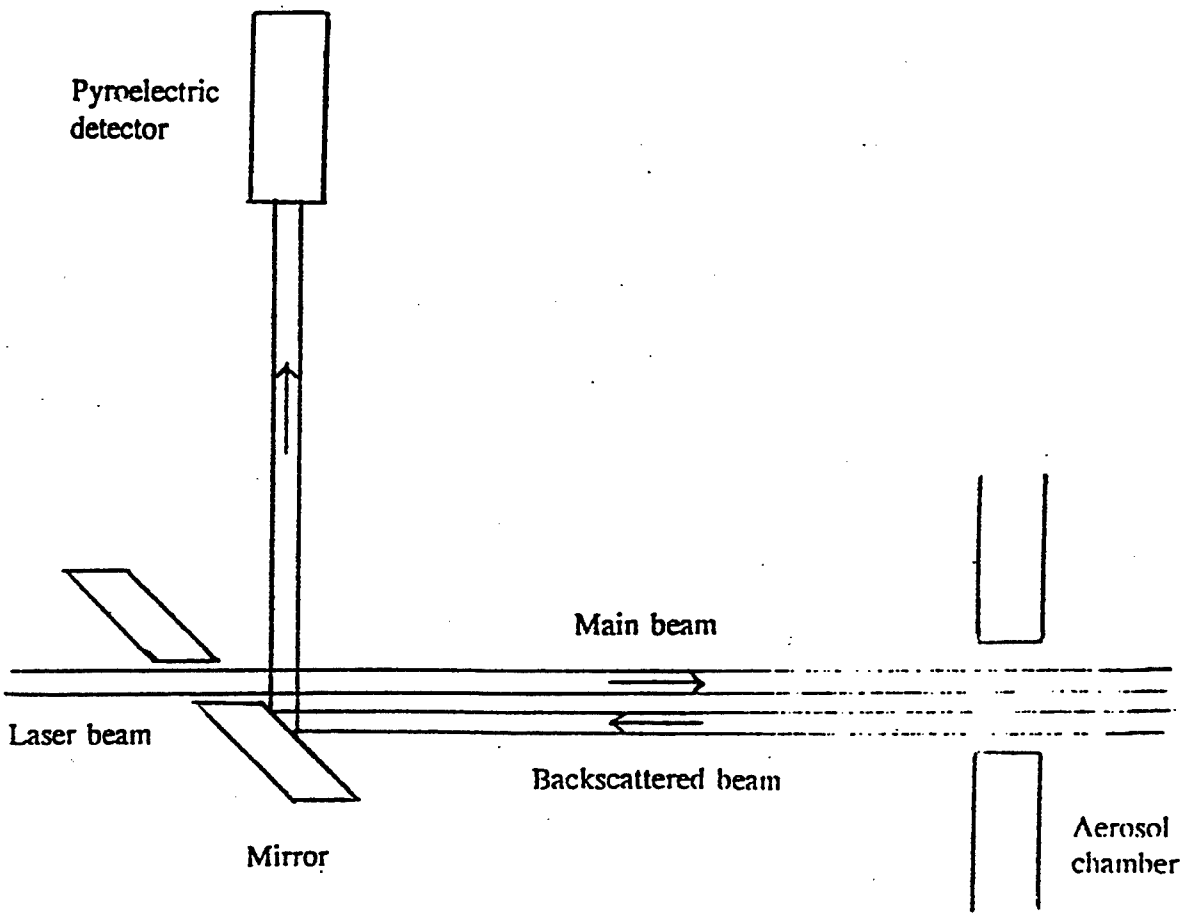

Figure 6. Schematic Diagram of Experimental Arrangement for Transmission and Backscatter Measurements.

The standard Mie values for extinction, Qe and backscatter efficiency, G, (assuming spheres) for the carbon graphite flakes (Asbury M260 # 4676) at 1064, 532, 355 and 266 nm wavelengths, λ, as a function of particle size parameter x (where $x = 2\pi r/\lambda$) are shown in Figures 7 and 8 respectively. The values of refractive index for carbon graphite flakes at each wavelength are given in Table 4.

Table 4. Extinction and Backscatter from Carbon Graphite Flakes (Asbury M260 # 4676).

Wavelength	Refractive Index (a) Real n	(b) Imaginary k	R	σ_e/σ_b sr (theoretical) (a) radius range 0.75 to 10 μm	(b) Geometric mean radius r_g = 1.2 μm	σ_e/σ_b sr (experimental)	Number of measurements
266	1.39	0.99	1.6	160 → 171	166	126(± 17)	74
355	1.57	0.76	2.4	216 → 235	225	173(± 15)	137
532	1.64	0.84	2.6	185 → 215	204	228(± 24)	81
1064	1.89	1.27	4.3	109 → 141	133	243(± 13)	80

The carbon graphite aerosol consisted of a polydispersion of particles having a lognormal distribution with sizes ranging from 0.75 to over 10 um radius with a numerical mean radius of 1.25 um. In each case, the size parameter was such that the backscatter and extinction values fell in the relatively constant region leading to asymptotic values of G and Qe.

In this case the backscatter gain, G_∞ is given by

$$G_\infty = \frac{(n-1)^2 + k^2}{(n+1)^2 + k^2} \tag{4}$$

where n and k and the real and imaginary indices of refraction.

The asymptotic values of Qe and G lead to the following appealingly simple theoretical form independent of size distribution given by:

$$\frac{\sigma_e}{\sigma_b} = \frac{4\pi Q_e}{G_\infty} \tag{5}$$

The theoretical Mie values for σ_e/σ_b for spheres shown in Table 1 were computed for the geometric mean radius of 1.2 μm and over the radius range 0.75 to 10 μm.

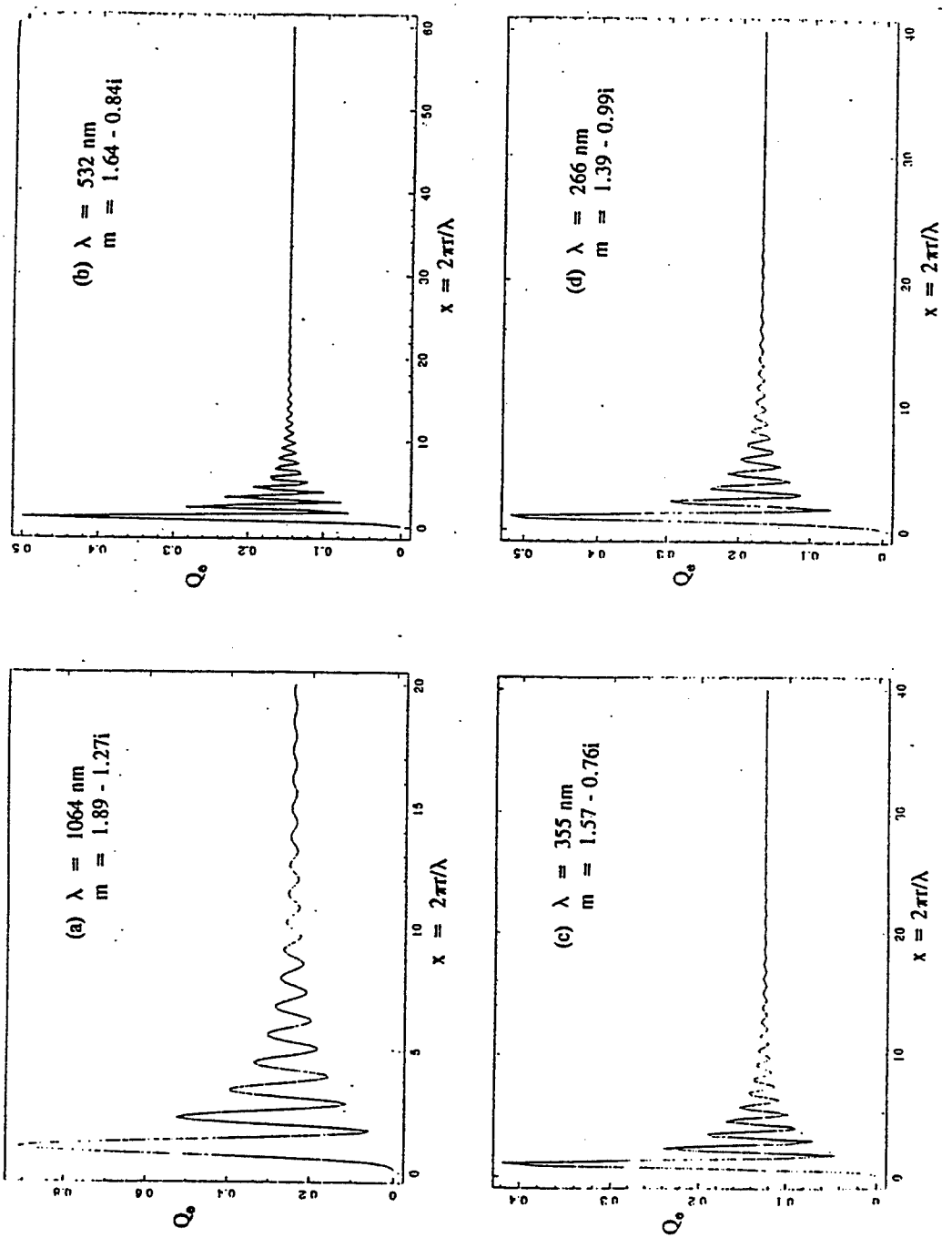

Figure 7. Mie Efficiency Factor for Extinction Qe as a Function of Particle Size Parameter x for Carbon Graphite Flakes (Asbury M260 #4676) at Different Wavelengths and Indices of Refraction, m.

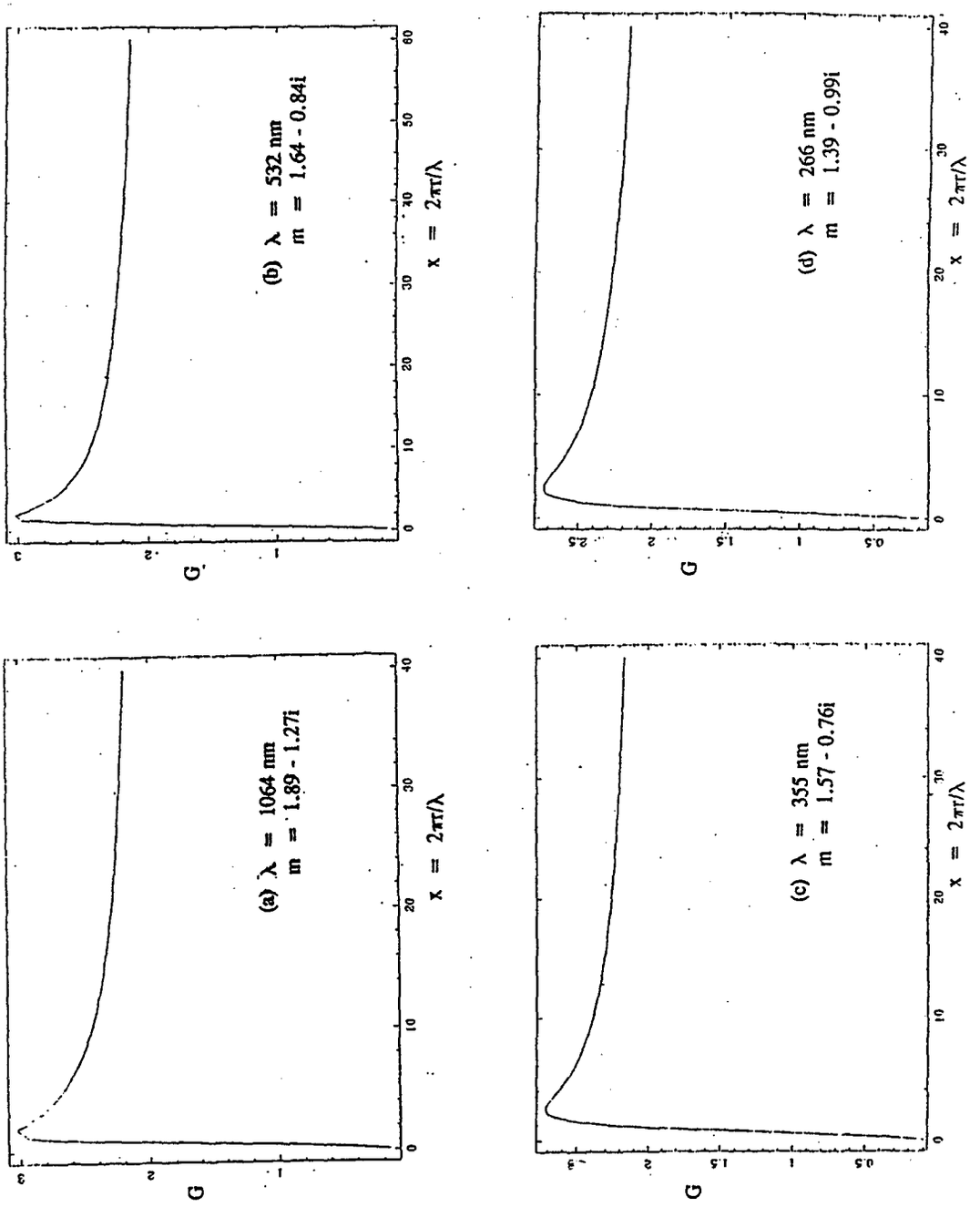

Figure 8. Mie Backscatter Gain G(m,x) as a Function of Particle Size Parameter x for Carbon Graphite Flakes (Asbury M260,#4676) at Different Wavelengths and Indices of Refraction, m.

5. SUMMARY AND CONCLUSIONS

The values for $\delta e < 0.1$ m-1 (corresponding to an aerosol mass density of < 0.056 g/m3) have large errors due to the low levels of backscattered signal observed. The values for $\delta e > 1$ m-1 (aerosol mass density > 0.56 g/m3) include multiple scattering effects whereas the theoretical values assume single scattering. Reasonably good agreement was obtained between the experimental and theoretical values for $\delta e/\delta b$ for obscuring aerosol of carbon graphite flakes (Asbury M260 # 4676) at 1064,532,355 and 266 nm.

Some consideration has been given to the effect of the shape of the carbon graphite flakes. The absorption of an infinite but thin slab with parallel sides in the Rayleigh limit (ie. for small particles whose diameter is much less than wavelength λ) has been determined by Faxvog and Roessler (1981). This slab can also be considered as a large thin disc. The ratio R of the absorption cross section per unit volume for slabs to the absorption cross section per unit volume for spheres (Mie) is given by I m^2 + 2 l^2/9 where refractive index m = n - ik. This ratio R is given in Table 4 for carbon graphite flakes (Asbury M260 # 4676) at 1064, 532, 355 and 266 nm wavelengths and is calculated to be 4.3, 2.6, 2.4 and 1.6 respectively. Incident light on a carbon graphite flake is absorbed, transmitted or scattered. An increase in absorption for a disc shaped particle results in a decrease in scattering for that same aerosol particle. This in return will result in a reduced value of backscatter.

This effect is expected to be more dominant at larger wavelengths for a given aerosol since proportionally more Rayleigh scatterers will be present. The sizes were only measured down to 0.75 um radius although some smaller Rayleigh particles would be expected. For absorbing aesosols Faxvog and Roessler (1981) have shown that maximum Mie scattering for spheres occurs in the range $0.15 < 2r < 0.5\lambda$,i.e. for particle radius ranging from 0.16 to 0.53 um at 1064 nm and from 0.040 to 0.13 um at 266 nm wavelength.

The experimental values for $\delta e/\delta b$ are greater than the theoretical values for spheres for carbon graphite flakes at the longer wavelengths 1064 and 532 nm as shown in Table 4. At the shorter wavelengths 355 and 266 nm the effect would not be expected as there are fewer Rayleigh scatterers. These results are consistent with the assumption that the carbon graphite flakes have a shape between that of spheres and infinite thin parallel slabs or large thin discs.

LITERATURE CITED

A. Deepak and M.A. Box, "Forward Scattering Corrections for Optical Extinction Measurements in Aerosol Media, 2: Polydispersions," Appl. Opt. 17, 3169 - 3176 (1978).

F.R. Faxvog and D.M. Roessler, "Optical Absorption in Thin Slabs and Spherical Particles," Appl. Opt. 20, 729 - 731 (1981).

F.R. Faxvog and D.M. Roessler, "Carbon Aerosol Visibility vs. Particle Size Distribution", Appl. Opt. 17, 2612 - 2616 (1978).